JOURNAL OF SOLID STATE CHEMISTRY 75, 270–278 (1988)

The High-Temperature Eu_2O_3–$BaCO_3$–CuO–Atmospheric Oxygen Phase Diagram: Phase Characterization in the 90 K Superconducting Region

S. A. HODOROWICZ,* A. LASOCHA,* W. LASOCHA,*
AND H. A. EICK†

Department of Chemistry, Michigan State University, East Lansing, Michigan 48824-1322

Received November 30, 1987; in revised form February 12, 1988

A comprehensive study of the Eu_2O_3–CuO–$BaCO_3$ (950°C $BaCO_3$ decomposition products) system has been effected on intimately mixed specimens which were subsequently fired both in air and in pure oxygen. In the binary oxide regions the phases Eu_2BaO_4, Eu_2CuO_4, and $BaCuO_{2+x}$ were observed. In the ternary oxide region the phases Eu_2BaCuO_5, $EuBa_2Cu_3O_{6.5+x}$, and $Eu_3Ba_3Cu_6O_{13.5+x}$ were observed. The phases were characterized by X-ray diffraction; structure type and lattice parameter data are reported. Only for $EuBa_2Cu_3O_{6.5+x}$ in the orthorhombic modification was 90 K superconductivity observed.

Introduction

Bednorz and Mueller's (*1*) report of a high-temperature layered perovskite-type superconducting phase has led to an intensive effort to characterize this family of materials. Even though superconductivity has been found in the multi- and single-phase metallic oxide systems, X–Ba–Cu–O (X = Y, La, Nd, Sm, Eu, Gd, Tb, Ho, Er, Tm, Yb, and Lu) (*2–10*), the phase diagrams of only a limited number of these systems have been examined in a systematic manner over the full composition range. The $YO_{1.5}$–BaO–CuO system has been examined most extensively (*11–18*). Although the superconducting properties of the $XBa_2Cu_3O_{6.5+x}$ oxide appear to be minimally affected by the choice of lanthanoid ion (*19*), the phases present in the M_2O_3–CuO–BaO system could change appreciably as M is varied. In an attempt to provide phase data which could help to clarify the structural relationships between systems with different M, a comprehensive study of the Eu_2O_3–CuO–d.p. $BaCO_3$ (950°C $BaCO_3$ decomposition products) system was undertaken. The choice of europium as a trivalent ion is somewhat arbitrary, but its ionic radius, which is slightly larger than that of yttrium and less than that of lanthanum, and its location near the middle of the lanthanoids suggested it to be a reasonable first choice.

After this work was completed, we became aware of phase studies on the closely

---

* On leave from the Faculty of Chemistry, Jagiellonian University, Poland.

† To whom correspondence should be addressed.

0022-4596/88 $3.00

related $LaO_{1.5}$–BaO–CuO (*20*) and $LaO_{1.5}$–SrO–CuO (*21*) systems, and of a phase study of the CuO-rich region of the $GdO_{1.5}$–BaO–CuO system (*22*). Indeed, the phases observed in the La–Ba—Cu–O system do in fact differ from those found for the Eu–Ba–Cu–O system and from those observed in the La–Sr–Cu–O system.

Experimental

Reactants were $BaCO_3$ (reagent grade, J. T. Baker Co., Phillipsburg, NJ), Eu_2O_3 (99.9%, Research Chemicals, Phoenix, AZ), and CuO (reagent grade, Mallinckrodt, St. Louis, MO). All reagents were analyzed by X-ray powder diffraction and found to be monophasic. Reactants, mixed in the appropriate molar quantities, were ground under acetone. The pulverized mixtures were then placed in platinum crucibles, oven dried at 150°C for ~2 hr, fired at 950°C in air for 24 hr, and then cooled at a rate of ~100°C hr^{-1}. Products obtained at this stage of reaction were examined by X-ray diffraction as described below. Some specimens were reground, fired again at 950°C for 12 hr in a stream of flowing O_2, cooled to ambient temperature at a rate of ~50°C hr^{-1} and examined again by X-ray diffraction. The platinum container was monitored carefully to ensure the absence of interference with the reactants. All products were examined for evidence of the Meissner effect by suspending them in liquid nitrogen in the presence of the magnetic field of a strong permanent magnet. The magnetic behavior of selected specimens was determined at 5 K in an SHE Corp. SQUID.

Phase analysis and characterization were effected by the Guinier X-ray powder diffraction technique with monochromatized Cu$K\alpha_1$ radiation in a 114.59-mm diameter camera evacuated to 10^{-3} Torr during exposure. NBS-certified Si powder [a = 5.43082(3) Å] served as the internal standard. Reflection positions were determined with a Supper film reader; intensities were estimated visually. For some products X-ray diffraction intensities were also measured at a scan rate of 2.5 sec/0.02° in 2θ with Cu$K\alpha$ radiation on a Philips APD 3720 diffractometer system fitted with a sample spinner, a θ-compensating slit, and a diffracted beam monochromator. These intensities were multiplied by the factor sin θ^{-1} to correct for the θ-compensating slit.

The program ITO9 (*23*) was used for indexing the observed reflections and APPLEMAN (*24*) for refining lattice parameters. X-ray powder diffraction intensities were calculated with the program POWD12 (*25*); positional and thermal parameters were taken from literature references. All calculations were effected on a VAX 11/750 computer.

Results and Discussion

The phase relationships in this system are presented in Fig. 1. The experimental data points necessary for establishing the phase diagram are summarized in Table I

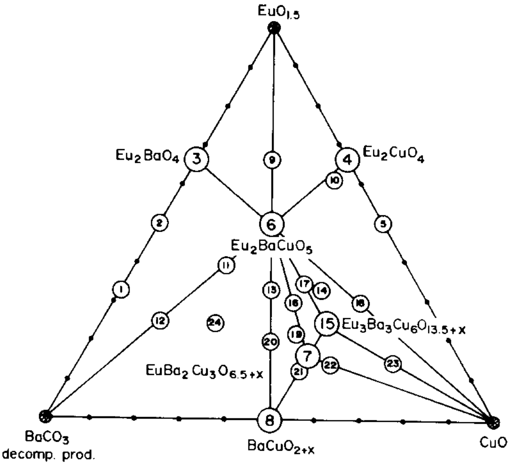

FIG. 1. The $EuO_{1.5}$–d.p.$BaCO_3$ (950°C decomposition products)–CuO phase diagram. The sides of the triangle are marked at 10-mole% intervals. The numbers on the points correspond to those listed in Table I.

TABLE I

PHASE RELATIONSHIPS IN THE $EuO_{1.5}$–d.p. $BaCO_3$–CuO SYSTEM

No.	Composition (mole ratio)	Expected phase	Products	Color[b]
1	33.3 : 66.7 : 0.0	$Eu_2Ba_4O_7$	Eu_2BaO_4 + d.p. $BaCO_3$[a]	White
2	50.0 : 50.0 : 0.0	$Eu_2Ba_2O_5$	Eu_2BaO_4 + d.p. $BaCO_3$[a]	White
3	66.7 : 33.3 : 0.0	Eu_2BaO_4	Eu_2BaO_4	White
4	66.7 : 0.0 : 33.3	Eu_2CuO_4	Eu_2CuO_4	Black
5	50.0 : 0.0 : 50.0	$Eu_2Cu_2O_5$	Eu_2CuO_4 + CuO	Black
6	50.0 : 25.0 : 25.0	Eu_2BaCuO_5	Eu_2BaCuO_5	Green
7	16.7 : 33.3 : 50.0	$EuBa_2Cu_3O_{6.5}$	$EuBa_2Cu_3O_{6.5+x}$	Black
8	0.0 : 50.0 : 50.0	$BaCuO_2$	$BaCuO_{2+x}$	Black
9	66.7 : 16.7 : 16.7	Eu_4BaCuO_8	Eu_2BaCuO_5 + Eu_2O_3	Sea green
10	61.7 : 5.0 : 33.3	$Eu_{1.85}Ba_{0.15}CuO$	Eu_2CuO_4 + Eu_2BaCuO_5	Black with green
11	40.0 : 40.0 : 20.0	$Eu_2Ba_2CuO_6$	Eu_2BaCuO_5 + d.p. $BaCO_3$[a]	Green
12	25.0 : 62.5 : 12.5	$Eu_2Ba_5CuO_9$	Eu_2BaCuO_5 + d.p. $BaCO_3$[a]	Sea green
13	33.3 : 33.3 : 33.3	$EuBaCuO_{3.5}$	Eu_2BaCuO_5 + probably $BaCuO_{2+x}$	Green and black
14	33.3 : 22.2 : 44.5	$Eu_3Ba_2Cu_4O_{10.5}$	Eu_2BaCuO_5 + $Eu_3Ba_3Cu_6O_{13.5+x}$	Green and black
15	25.0 : 25.0 : 50.0	$Eu_3Ba_3Cu_6O_{13.5+x}$	$Eu_3Ba_3Cu_6O_{13.5+x}$	Black
16	30.0 : 30.0 : 40.0	$Eu_{1.5}Ba_{1.5}Cu_2O_{5.75}$	Eu_2BaCuO_5 + $EuBa_2Cu_3O_{6.5+x}$	Green and black
17	35.0 : 25.0 : 40.0	$Eu_{3.5}Ba_{2.5}Cu_4O_{11.75}$	Eu_2BaCuO_5 + $Eu_3Ba_3Cu_6O_{13.5+x}$	Green and black
18	30.0 : 15.0 : 55.0	$Eu_3Ba_{1.5}Cu_{5.5}O_{11.5}$	Eu_2BaCuO_5 + CuO	Green and black
19	22.2 : 33.3 : 44.5	$Eu_2Ba_3Cu_4O_{10}$	Eu_2BaCuO_5 + $EuBa_2Cu_3O_{6.5+x}$	Black and green
20	25.0 : 37.5 : 37.5	$Eu_2Ba_3Cu_3O_9$	Eu_2BaCuO_5 + $BaCuO_{2+x}$	Black and green
21	12.5 : 37.5 : 50.0	$EuBa_3Cu_4O_{8.5}$	$EuBa_2Cu_3O_{6.5+x}$ + probably $BaCuO_{2+x}$	Black
22	14.3 : 28.6 : 57.1	$EuBa_2Cu_4O_{7.5}$	$EuBa_2Cu_3O_{6.5+x}$ + CuO	Black
23	15.0 : 15.0 : 70.0	$Eu_{1.5}Ba_{1.5}Cu_7O_{10.75}$	$Eu_3Ba_3Cu_6O_{13.5+x}$ + CuO	Black
24	25.0 : 50.0 : 25.0	$Eu_3Ba_6Cu_3O_{13.5}$	Eu_2BaCuO_5 + $BaCuO_{2+x}$	Green and black

[a] Products of $BaCO_3$ decomposition at 950°C.

[b] Predominant color listed first.

together with mixed composition, expected phase(s), observed phase(s), and specimen color. Under the experimental conditions used six compounds are formed: Eu_2BaO_4, Eu_2CuO_4, $BaCuO_{2+x}$, Eu_2BaCuO_5, $EuBa_2Cu_3O_{6.5+x}$, and $Eu_3Ba_3Cu_6O_{13.5+x}$. They are indicated in bold type in the phase diagram (Fig. 1). Lattice parameter data for all observed phases and some literature data on these and related phases are presented in Table II.

The Binary Regions

In the binary Eu_2O_3–d.p. $BaCO_3$ region dieuropium barium oxide, Eu_2BaO_4, was

TABLE II

CRYSTALLOGRAPHIC DATA ON COMPOUNDS OBTAINED IN THE $EuO_{1.5}$–d.p. $BaCO_3$–CuO SYSTEM

Composition	Symmetry[a]	Lattice parameters[b]			Ref.[c]	Remarks
		a (Å)	*b* (Å)	*c* (Å)		
Eu_2BaO_4	O	10.508(3)	3.538(1)	12.285(3)		
Eu_2CuO_4	T	3.900(1)		11.902(2)		
		3.895		11.887	(*26*)	
		3.907		11.917	(*27*)	
		3.901(1)		11.897(3)		In $Eu_{1.85}Ba_{0.15}$ CuO_4 sample
Eu_2BaCuO_5	O	7.231(3)	12.339(1)	5.734(1)		
		7.243(2)	12.356(4)	5.740(3)	(*28*)	
$EuBa_2Cu_3O_{6.5+x}$	O	3.857(2)	3.900(2)	11.749(5)		Initial heating
		3.840(2)	3.900(2)	11.712(4)		After heating in O_2
		3.869(2)	3.879(3)	11.693(6)	(*29*)	
$BaCuO_{2+x}$	O	9.925(7)	5.642(5)	4.749(3)		Initial heating
	T	3.8634(3)		11.563(2)		After heating in O_2
$BaCoO_{2.93}$	O	9.780	5.627	4.758	(*30*)	
$Eu_3Ba_3Cu_6O_{13.5-x}$	T	3.8610(4)		11.568(2)		Initial heating
	O	9.911(1)	5.625(8)	4.755(8)		After heating in O_2
$La_3Ba_3Cu_6O_{14.1}$		5.5253(5)		11.721(1)	(*31*)	$a/\sqrt{2} = 3.9069$

[a] O, orthorhombic; T, tetragonal.

[b] The estimated standard deviations (in parentheses) refer to the last digit indicated.

[c] This work except as noted.

obtained as a white sintered compact. Its X-ray powder diffraction pattern (Table III) was indexed best with a cell of orthorhombic symmetry; derived lattice parameters are very close to those reported for Y_2BaO_4 (*32*). Similar interplanar *d*-spacings were reported by Barry and Roy (*33*) for Gd_2BaO_4 (see Table III), but the diffraction data were not indexed. Comparison of the observed diffraction intensities to those calculated with the atomic coordinates and thermal parameters reported for $CoFe_2O_4$ (*34*) confirm that the phase has a spinel type of structure.

Three additional phases, $Ba_2Y_2O_5$, $Ba_3Y_4O_9$, and $Ba_4Y_2O_7$, were reported by Kwestroo *et al.* (*32*) in the closely related binary Y_2O_3–BaO system. However, samples of Eu_2O_3 and $BaCO_3$ mixed in molar ratios appropriate for synthesis of these three phases did not produce a single phase, but mixtures of Eu_2BaO_4 and d.p. $BaCO_3$. These 950°C $BaCO_3$ decomposition products consisted of a mixture of BaO and $Ba(OH)_2 \cdot H_2O$ (*35*) when the sample was decomposed and cooled slowly in air. They were a mixture of BaO and BaO_2 when the sample was decomposed in air, quenched, and then transferred under dry Ar to a glove box whose Ar atmosphere was continuously purged of moisture by passage through molecular sieves.

In the binary Eu_2O_3–CuO system only one perovskite-type phase, Eu_2CuO_4, was identified; its diffraction pattern and tetragonal unit cell parameters (Table II) correlate well with literature values (*26*, *27*). The stable X_2CuO_5-type phase whose existence was quoted by Steinfink *et al.* (*11*) from JCPDS X-ray diffraction file reports (*36*) was not observed.

In the binary CuO–d.p. $BaCO_3$ region the final product obtained by heating an equimolar mixture of CuO and $BaCO_3$ at 950°C

TABLE III

OBSERVED AND CALCULATED INTERPLANAR *d*-SPACINGS (Å) AND INTENSITY DATA FOR THE PHASES, Ln_2BaO_4, Ln = Eu AND Gd

Eu_2BaO_4					Gd_2BaO_4 (*33*)	
d_o	d_c	$h\ k\ l$	I_o	I_c[a]	d	I/I_o
5.264	5.254	2 0 0	1	5.0		
3.995	3.993	2 0 2	5	8.6		
3.401	3.400	0 1 1	8	9.1		
3.236	3.235	1 1 1	8	8.3		
3.072	3.071	0 0 4	47	46.4	3.06	58
3.044	3.043	3 0 2	100	100.0	3.03	100
2.947	2.948	1 0 4	67	7.7		
	2.943	1 1 2		72.3	2.92	54
2.935	2.935	2 1 0	33	34.4		
2.855	2.854	2 1 1	8	5.6	2.83	14
2.594	2.594	1 1 3	26	21.6	2.58	13
2.441	2.439	3 1 1	13	7.9	2.42	18
2.415	2.415	4 0 2	5	3.6		
2.386	2.385	2 1 3	5	0.9	2.36	12
2.306	2.307	3 1 2	2	3.2		
2.264	2.265	1 1 4	7	8.7	2.24	10
2.122	2.127	3 1 3	40	8.6		
	2.122	2 1 4		31.4	2.11	90
2.108	2.109	4 1 0	27	20.6		
2.078	2.078	4 1 1	10	10.7		
2.018	2.018	0 1 5	6	4.3	2.01	15
1.9079	1.9077	2 0 6	12	11.2	1.906	14
1.8839	1.8839	2 1 5	7	4.2		
1.7683	1.7690	0 2 0	48	18.5	1.765	32
	1.7676	3 0 6		14.8		
1.7475	1.7475	1 1 6	34	15.8		
1.7388	1.7386	4 1 4	29	21.3	1.731	58
1.6789	1.6792	2 1 6	9	6.3		
1.6528	1.6531	5 1 3	6	2.3		
1.6154	1.6149	4 0 6	6	3.1	1.613	18
1.5998	1.6004	4 1 5	6	3.0		
1.5694	1.5695	6 1 0	3	1.8		
1.5547	1.5548	1 1 7	6	3.1		
1.5322	1.5329	0 2 4	21	13.8		
1.5290	1.5293	3 2 2	43	30.8		
1.5208	1.5213	6 0 4	18	12.3		

[a] Intensities calculated with atomic parameters given in (*33*) for $CaFe_2O_4$.

in air is black $BaCuO_{2+x}$. Its diffraction pattern could be indexed on orthorhombic symmetry and it possessed a magnetic moment as evidenced by its behavior in a strong magnetic field. Similar observations were reported for a $BaCuO_{2.5}$ phase prepared by heating an equimolar mixture of BaO_2 and $Cu(NO_3)_2$ at 580°C in air (*37*). These observations suggest the presence of copper(III) ions in the specimen. The observed powder diffraction pattern (Table IV) is in good agreement with that reported (*38*) for the barium cobalt oxide, $BaCoO_{2.8}$, with lattice parameters very close to those of the $BaCoO_{2.93}$ phase described in (*30*) (Table II). When this barium copper oxide was heated again at 950°C under a dynamic oxygen atmosphere, it transformed into a new modification (Table IV) which could be indexed on tetragonal symmetry. Neither of these Ba–Cu–O phases evidenced the Meissner effect at liquid nitrogen temperatures.

The Ternary Region

In the ternary region three phases, Eu_2BaCuO_5, $EuBa_2Cu_3O_{6.5+x}$ ("123"), and $Eu_3Ba_3Cu_6O_{13.5+x}$ ("336"), were characterized. All were obtained pure and were completely devoid of reflections characteristic of the reactants. The diffraction pattern of the green Eu_2BaCuO_5 (Table V) evidences orthorhombic symmetry with lattice parameters very close to those reported by Michel and Raveau (*28*). Even though the Eu_2BaCuO_5 specimen was ground and fired two times under a dynamic oxygen atmosphere, its diffraction pattern did not

TABLE IV

OBSERVED AND CALCULATED INTERPLANAR *d*-SPACINGS (Å) AND OBSERVED INTENSITY DATA FOR THE ORTHORHOMBIC AND TETRAGONAL MODIFICATIONS OF $BaCuO_{2+x}$ PHASES

Orthorhombic modification				Tetragonal modification			
d_o	d_c	$h\ k\ l$	I_o[a]	d_o	d_c	$h\ k\ l$	I_o[a]
3.712	3.726	2 1 0	vw	11.56	11.54	1 0 1	w
3.405	3.411	1 1 1	s	3.864	3.863	1 0 0	m
3.310	3.308	3 0 0	s	3.212	3.212	1 0 2	vw
2.858	2.854	3 1 0	s	2.729	2.732	1 1 0	vs
2.823	2.821	0 2 0	vs		2.729	1 0 3	
2.374	2.374	0 0 2	w	2.313	2.314	1 0 4	m
2.270	2.271	4 1 0	vw	2.228	2.229	1 1 3	m
2.178	2.179	2 2 1	m	1.9320	1.9317	2 0 0	s
2.138	2.137	1 1 2	w	1.7278	1.7278	2 1 0	w
1.7051	1.7058	2 2 2	vw	1.7090	1.7088	2 1 1	vw
1.5082	1.5080	2 0 3	vw	1.5765	1.5766	2 1 3	s
1.4586	1.4582	1 3 2	vw	1.4833	1.4831	2 1 4	m
1.4126	1.4131	2 3 2	vw	1.3644	1.3643	2 0 6	m

[a] Estimated from Guinier films.

TABLE V

OBSERVED AND CALCULATED INTERPLANAR *d*-SPACING (Å) AND INTENSITY DATA FOR THE PHASE Eu_2BaCuO_5

d_0	d_c	*h k l*	I_0	I_c^a
4.481	4.492	1 0 1	4	8.8
3.615	3.615	2 0 0	2	1.8
3.464	3.469	2 1 0	6	9.5
3.084	3.084	0 4 0	3	1.3
3.031	3.033	1 3 1	100	100.0
2.966	2.968	2 1 1	67	67.4
2.867	2.867	0 0 2	48	53.1
2.837	2.837	1 4 0	22	28.4
2.740	2.740	2 2 1	12	10.0
2.713	2.715	2 3 0	8	9.5
2.543	2.543	1 4 1	10	9.3
2.454	2.454	2 3 1	11	9.4
2.365	2.365	3 1 0	5	4.2
2.335	2.335	1 5 0	10	8.5
2.246	2.245	3 2 0	24	16.8
2.222	2.222	3 0 1	11	13.3
2.208	2.210	2 1 2	12	11.8
2.186	2.186	3 1 1	7	4.9
2.165	2.163	1 5 1	5	4.2
2.100	2.100	0 4 2	6	3.8
2.056	2.056	0 6 0	5	6.5
2.016	2.016	1 4 2	45	39.5
1.9715	1.9715	2 3 2	15	13.2
1.9558	1.9550	3 3 1	3	3.3
1.9356	1.9357	0 6 1	1	0.6
1.9000	1.8994	3 4 0	18	14.2
1.8706	1.8699	1 6 1	5	4.0
1.8110	1.8108	1 5 2	13	6.2
1.7880	1.7875	2 6 0	7	4.8
1.7678	1.7676	3 2 2	18	14.8
1.7126	1.7125	1 7 0	6	4.5
1.7076	1.7075	4 1 1	8	6.4

[a] Intensities calculated with atomic coordinates given in (*28*).

change and it was paramagnetic even at 5 K. It should be noted that the structure of the Eu_2BaCuO_5 phase (*28*) is distinctly different from that of the $XBa_2Cu_3O_{6.5+x}$ superconducting phase (*39*).

Reactants in the mole ratio Eu : Ba : Cu = 1 : 2 : 3, when heated in air, produced a black product which did not show the Meissner effect at liquid nitrogen temperatures. It has been postulated (*40*) that slow cooling of the samples to room temperature stabilizes the superconducting orthorhombic phase while fast cooling and quenching leads to a nonsuperconducting state. However, "123" samples prepared by both procedures yielded identical lattice parameters and no Meissner effect at liquid nitrogen temperatures. The superconducting "123" phase was produced by heating these orthorhombic symmetry specimens in a dynamic oxygen atmosphere at 950°C and cooling them slowly (50°C hr^{-1}). The Meissner effect now was observed at liquid nitrogen temperatures, even though diffraction patterns of both the superconducting and nonsuperconducting phases were in practice the same (Table VI); both showed the characteristic orthorhombic splittings. The refined lattice parameters of the superconducting phase are slightly smaller (Table II) than those of the nonsuperconducting phase, probably because of a slight change in the copper ion oxidation state. This result contrasts with that of Appelman *et al.* (*40*) who observed in the $YBa_2Cu_3O_x$ orthorhombic phase a large variation in oxygen content without a concomitant lattice parameter change.

The black product resulting from mixture number 15 ("336," Table I) was monophasic and corresponded very well, as can be seen in Table II, to the tetragonal $La_3Ba_3Cu_6O_{14.1}$ phase described by Er-Rakho *et al.* (*31*) when their *a* parameter is transformed to our smaller parameter. X-ray diffraction data for this phase are presented in Table VII. This "336" sample, when in a strong magnetic field, did not show the Meissner effect typical of the "123" superconducting phase. However, after it had been heated at 950°C under a dynamic oxygen atmosphere, the "336" sample was paramagnetic at 5 K and evidenced a diffraction pattern (Table VII) which was indexable on orthorhombic symmetry; refined lattice parameters are presented in Table II. Some of

TABLE VI

OBSERVED AND CALCULATED INTERPLANAR d-SPACING (Å) AND INTENSITY DATA FOR THE 90 K $EuBa_2Cu_3O_{6.5+x}$ SUPERCONDUCTING PHASE

d_o	d_c	$h\ k\ l$	I_o	I_c[a]
11.74	11.74	0 0 1	16	22.3
3.911	3.916	0 0 3	10[b]	10.4
	3.900	0 1 0		12.0
3.857	3.857	1 0 0	3	7.6
3.670	3.665	1 0 1	1	2.7
3.247	3.249	0 1 2	vvw[c]	0.6
3.225	3.224	1 0 2	2	2.3
2.764	2.763	0 1 3	51	89.8
2.744	2.748	1 0 3	100	100.0
	2.742	1 1 0		97.7
2.485	2.485	1 1 2	vvw[c]	0.1
2.348	2.349	0 0 5	10	6.3
	2.346	0 1 4		10.4
2.335	2.336	1 0 4	6	7.7
2.245	2.246	1 1 3	28	30.3
2.006	2.006	1 0 5	3	0.2
	2.004	1 1 4		2.6
1.9590	1.9582	0 0 6	32	18.2
1.9503	1.9500	0 2 0		31.7
1.9281	1.9285	2 0 0	15	30.7
1.7845	1.7843	1 1 5	3	3.1
1.7492	1.7499	0 1 6	7	3.3
1.7449	1.7460	1 0 6	6	2.4
	1.7456	0 2 3		3.0
1.7308	1.7301	2 0 3	5	2.9
1.5925	1.5936	1 1 6	64[b]	37.7
	1.5903	1 2 3		45.6
1.5815	1.5815	2 1 3	25	40.9
1.4998	1.5005	0 2 5	3	3.2
1.4894	1.4898	2 1 4	5	5.5
1.4320	1.4316	1 1 7	5	6.3
1.3815	1.3817	0 2 6	11	47.8
1.3733	1.3740	2 0 6	30	12.8
1.3709	1.3712	2 2 0		21.7
1.2947	1.2959	2 1 6	9	3.0
	1.2942	2 2 3		2.8
1.2333	1.2338	0 3 3	15	10.1
	1.2319	1 3 0		11.1
1.2208	1.2215	3 0 3	18	10.6
	1.2210	3 1 0		10.8
1.1754	1.1751	1 3 3	3	4.3
1.1234	1.1239	1 0 10	2	3.3
	1.1232	2 2 6	10	14.0
	1.1224	1 2 8	2	3.6

[a] Intensities were calculated with atomic coordinates given for $YBa_2Cu_3O_{7-y}$ in (*39*).

[b] Broad line.

[c] Very, very weak line. Estimated from a Guinier film.

the X-ray reflections were broad and could represent partial disorder. Alternately, this broadness could be reflective of an order–disorder phase transition between the two "336" structural modifications, and, as has been observed in $YBa_2Cu_3O_{7-x}$ (*41*), may result from continuous disordering of oxygen atoms into normally vacant sites. More likely though, the broadness simply reflects a continuous region of solid solution between the "123" and "336" compounds as has been observed in related systems (*21*).

In summary, our detailed investigations of the title system indicate the following:

(1) Six phases are present under the pressure and temperature conditions investigated. Attempts to prepare $Eu_2Y_2O_4$ (Y = Ba or Cu) phases were unsuccessful. Con-

TABLE VII

OBSERVED AND CALCULATED INTERPLANAR d-SPACINGS (Å) AND OBSERVED INTENSITY DATA FOR TWO MODIFICATIONS OF $Eu_3Ba_3Cu_6O_{13.5+x}$

Tetragonal modification				Orthorhombic modification			
d_o	d_c	$h\ k\ l$	I_o[a]	d_o	d_c	$h\ k\ l$	I_o[a]
11.53	11.56	0 0 1	w	3.434	3.431	2 0 1	w
3.849	3.856	0 0 3	m	3.409	3.409	1 1 1	s
3.209	3.211	1 0 2	w	2.923	2.929	2 1 1	w
2.727	2.728	1 0 3	vs	2.848	2.848	3 1 0	m
2.311	2.314	1 0 4	m	2.821	2.813	0 2 0	m
2.226	2.228	1 1 3	m	2.377	2.377	0 0 2	vvw
1.9845	1.9852	1 1 4	vw	2.192	2.197	4 0 1	w
					2.190	0 1 2	
1.9313	1.9305	2 0 0	s				
					2.143	2 0 2	
1.7647	1.7650	1 1 5	vw	2.138	2.141	3 2 0	w
					2.138	1 1 2	
1.7269	1.7267	2 1 0	m	2.046	2.046	4 1 1	w
	1.7262	2 0 3					
				1.8760	1.8750	0 3 0	vvw
1.5757	1.5759	2 1 3	s				
	1.5749	1 1 6		1.6542	1.6542	6 0 0	vvw
1.5192	1.5192	1 0 7	vw	1.6239	1.6231	5 2 0	vvw
1.4823	1.4825	2 1 4	w				
	1.4823	2 0 5					
1.3647	1.3651	2 2 0	m				
	1.3642	2 0 6					
1.2862	1.2870	3 0 0	w				
	1.2868	2 2 3					
	1.2863	2 1 6					
	1.2853	0 0 9					

[a] Estimated from Guinier films; v = very, m = medium, s = strong, w = weak.

sequently, this $EuO_{1.5}$–BaO–CuO phase diagram (Fig. 1) differs from that of the $YO_{1.5}$–BaO–CuO system reported, for example in (*11, 12, 14, 18*), all of which basically agree.

(2) In the ternary $EuO_{1.5}$–BaO–CuO system some of the single phases reported for other systems were not observed. There are numerous reports of superconductivity for $La_{2-x}(Ba, Sr)_xCuO_4$ phases. Sample 10 (Fig. 1), which had a mixed composition of $Eu_{1.85}Ba_{0.15}CuO_4$, was a mixture of Eu_2BaCuO_5 and Eu_2CuO_4 phases. An $Eu_{1.5}Ba_{1.5}Cu_2O_x$ specimen was also reported to be diphasic (*42*). The $LaBaCu_2O_{5+x}$ and $La_2BaCu_2O_6$ phases reported (*43*) to be pure compounds appear from (*21*) to be but members of an extended solid solution region.

The $EuO_{1.5}$–BaO–CuO and $GdO_{1.5}$–BaO–CuO systems also differ (*22*). Although the binary regions that can be compared agree well, only "211" and "123" ternary phases are observed in the Gd system. A "336" phase is not reported. In view of the close relationship between the ionic radii of Eu and Gd, such a difference is indeed surprising. It is apparent that the $MO_{1.5}$BaO–CuO phase diagrams differ significantly with differing M.

(3) The preparative results suggest that the orthorhombic modification of the superconducting phase can be obtained even when the specimen has not been heated under a pure oxygen atmosphere, but the oxygen content in the structure has a strong influence on whether the superconductivity will be observed at ~90 K. This observation suggests a direct relationship between the Cu(II) : Cu(III) ratio and the oxygen stoichiometry. Alternately, if the postulate of de Groot *et al.* (*44*), that the valence fluctuation present in mixed oxides requires dynamic peroxide formation is applicable, additional oxygen may be required to achieve the necessary anion proximity.

(4) These results help to clarify the role of the reactant, $BaCO_3$. Because this compound decomposes in air through the peroxide, BaO_2, it can either effect or influence the oxidation of Cu(II) to Cu(III). In addition, the presence of the large Ba(II) ion in the structure helps to stabilize the Cu(III) ions.

(5) The heating of the initial $BaCuO_{2+x}$ and "336" phases in an oxygen atmosphere has a strong influence on their structure. The transformations in these phases probably are connected with the conversion of some Cu(II) ions to Cu(III).

It is now clear that the trivalent cation significantly affects system behavior even though in all cases the ~90 K superconducting "123" phase is observed. The superconducting and magnetic properties of some of the phases obtained in the title system will be reported elsewhere.

Acknowledgments

Support of the National Science Foundation, Division of Materials Research, Solid State Chemistry Program, DMR 84-00739, is acknowledged gratefully. S.A.H, A.L, and W.L. also acknowledge support of the Polish Academy of Science, Program CPBP 01.12.

References

1. J. G. Bednorz and K. A. Müller, *Z. Phys. B* **64,** 189 (1986).
2. M. K. Wu, J. R. Ashburn, C. J. Torng, P. H. Hor, R. L. Meng, L. Gao, Z. J. Huang, Y. Q. Wang, and C. W. Chu, *Phys. Rev. Lett.* **58,** 908 (1987).
3. J. Z. Sun, D. J. Webb, M. Naito, K. Char, M. R. Hahn, J. W. P. Hsu, A. D. Kent, D. B. Mitzi, B. Oh, M. R. Beasley, T. H. Geballe, R. H. Hammond, and A. Kapitulnik, *Phys. Rev. Lett.* **58,** 1574 (1987).
4. R. J. Cava, B. Batlogg, R. B. van Dover, D. W. Murphy, S. Sunshine, T. Siegrist, J. P. Remeika, E. A. Rietman, S. Zahurak, and G. P. Espinosa, *Phys. Rev. Lett.* **58,** 1676 (1987).
5. J. M. Tarascon, L. H. Greene, W. R. McKinnon, and G. W. Hull, *Phys. Rev. B* **35,** 7115 (1987).

6. P. M. Grant, R. B. Beyers, E. M. Engler, G. Lim, S. S. P. Parkin, M. L. Ramirez, V. Y. Lee, A. Nazzal, J. E. Vazquez, and R. J. Savoy, *Phys. Rev. B* **35,** 7242 (1987).
7. P. H. Hor, R. L. Meng, Y. Q. Wang, L. Gao, Z. J. Huang, J. Bechtold, K. Forster, and C. W. Chu, *Phys. Rev. Lett.* **58,** 1891 (1987).
8. D. W. Murphy, S. Sunshine, R. B. van Dover, R. J. Cava, B. Batlogg, S. M. Zahurak, and L. F. Schneemeyer, *Phys. Rev. Lett.* **58,** 1888 (1987).
9. S. R. Ovshinsky, R. T. Young, D. D. Allred, G. De Maggio, and G. A. Van der Leeden, *Phys. Rev. Lett.* **58,** 2579 (1987).
10. H. Takagi, S. Uchida, K. Kitazawa, and S. Tanaka, *Japan J. Appl. Phys.* **26,** L123 (1987).
11. H. Steinfink, J. S. Swinnea, Z. T. Sui, H. M. Hasu, and J. B. Goodenough, *J. Amer. Chem. Soc.* **109,** 3348 (1987).
12. L. Soderholm, D. W. Capone II, D. G. Hinks, J. D. Jorgensen, I. K. Schuller, J. Grace, K. Zhang, and C. U. Segre, *Inorg. Chim. Acta* **140,** 167 (1987).
13. D. G. Hinks, L. Soderholm, D. W. Capone II, J. D. Jorgensen, I. K. Schuller, C. U. Segre, K. Zhang, and J. Grace, *Appl. Phys. Lett.* **50,** 1688 (1987).
14. G. R. Wagner, J. Panson, and A. I. Braginski, *Phys. Rev. B.* **36,** 7124 (1987).
15. K. G. Frase and D. R. Clarke, *Adv. Ceram. Mater.* **2,** 295 (1987).
16. R. S. Roth, K. L. Davis, and J. R. Dennis, *Adv. Ceram. Mater.* **2,** 303 (1987).
17. G. Wang, S. J. Hwu, S. N. Song, J. B. Ketterson, D. L. Marks, K. R. Poeppelmeier, and T. O. Mason, *Adv. Ceram. Mater.* **2,** 313 (1987).
18. S.-J. Hwu, S. N. Song, J. B. Ketterson, T. O. Mason, and K. R. Poeppelmeier, *J. Amer. Ceram. Soc.* **70,** C165 (1987).
19. J. M. Tarascon, W. R. McKinnon, L. H. Greene, G. W. Hull, and E. M. Vogel, *Phys. Rev. B.* **36,** 226 (1987).
20. J. Hahn, T. O. Mason, S.-J. Hwu, and K. R. Poeppelmeier, private communication.
21. D. Klibanow, K. Sujata, and T. O. Mason, private communication.
22. J. K. Liang, X. T. Xu, G. H. Rao, S. S. Xie, X. Y. Shao, and Z. G. Duan, *J. Phys. D: Appl. Phys.* **20,** 1324 (1987).
23. J. W. Visser, *J. Appl. Crystallogr.* **2,** 89 (1969).
24. D. W. Appleman, D. S. Handwerker, and H. T. Evans, "Program X-Ray," Geological Survey, U.S. Department of the Interior, Washington, DC (1966).
25. D. K. Smith, M. C. Nichols, and M. E. Zolensky, "A FORTRAN IV Program for Calculating X-Ray Powder Diffraction Patterns, Version 10," Pennsylvania State University, University Park, PA (1983).
26. Powder Diffraction File, JCPDS: International Centre for Diffraction Data, 1601 Park Lane, Swarthmore, PA 19081, Data 1983, File No. 24-399.
27. Powder Diffraction File, JCPDS: International Centre for Diffraction Data, 1601 Park Lane, Swarthmore, PA 19081, Data 1983, File No. 22-34.
28. C. Michel and B. Raveau, *J. Solid State Chem.* **43,** 73 (1982).
29. T. Siegrist, S. A. Sunshine, L. F. Schneemeyer, D. W. Murphy, S. M. Zahurak, J. V. Waszczak, W. R. McKinnon, J. M. Tarascon, G. W. Hull, and L. H. Greene, *Phys. Rev. B* **36,** 3617 (1987).
30. M. Zanne, A. Courtois, and C. Gleitzer, *Bull. Soc. Chim. Fr.,* 4470 (1972).
31. L. Er-Rakho, C. Michel, J. Provost, and B. Raveau, *J. Solid State Chem.* **37,** 151 (1981).
32. W. Kwestroo, H. A. M. Van Hal, and C. Langereis, *Mater. Res. Bull.* **9,** 1631 (1974).
33. T. L. Barry and R. Roy, *J. Inorg. Nucl. Chem.* **29,** 1243 (1967).
34. B. F. Decker and J. S. Kasper, *Acta Crystallogr.* **10,** 332 (1957).
35. Powder Diffraction File, JCPDS: International Centre for Diffraction Data, 1601 Park Lane, Swarthmore, PA 19801, Data 1983, File No. 26-154.
36. Powder Diffraction File, JCPDS: International Centre for Diffraction Data, 1601 Park Lane, Swarthmore, PA 19801, Data 1983, File No. 33-511.
37. M. Arjomand and D. J. Machiu, *J. Chem. Soc. Dalton Trans.,* 1061 (1975).
38. B. E. Gushee, L. Katz, and R. Ward, *J. Amer. Chem. Soc.* **79,** 5601 (1957).
39. M. F. Garbauskas, R. H. Arendt, and J. S. Kasper, *Inorg. Chem.* **26,** 3191 (1987).
40. E. H. Appelman, L. R. Morss, A. M. Kimi, U. Geiser, A. Umezawa, G. W. Crabtree, and K. D. Carlson, *Inorg. Chem.* **26,** 3237 (1987).
41. J. D. Jorgensen, M. A. Beno, D. G. Hinks, L. Soderholm, K. J. Volin, R. L. Hitterman, J. D. Grace, I. K. Schuller, C. U. Segre, K. Zhang, and M. S. Kleefisch, *Phys. Rev. B* **36,** 3608 (1987).
42. D. W. Cooke, H. Rempp, Z. Fisk, J. L. Smith, and M. S. Jahan, *Phys. Rev. B* **36,** 2287 (1987).
43. S. Xie, C. Yang, X.-J. Wu, G. Che, H. Fan, W. Chen, Y. Zhou, Z. Zhao, Q. Yang, G. Chen, J. Liang, and F. Li, *Phys. Rev. B* **36,** 2311 (1987).
44. R. A. de Groot, H. Gutfreund, and H. Wagner, *Solid State Commun.* **63,** 451 (1987).